Online Resources

Microsatellites development, cross-amplification for *Aquilaria sinensis*, an endangered agarwood producing tree

ZHENG-FENG WANG[1], HONG-LIN CAO[1], CHU-XIONG CAI[2], YUN-GUO[1], ZHANG-MING WANG[1]

[1]Guangdong Provincial Key Laboratory of Applied Botany, South China Botanical Garden, Chinese Academy of Sciences, Guangzhou, China

[2]Dongguan Botanical Garden, Dongguan, China

Corresponding author:

Hong-Lin Cao

South China Botanical Garden,

Chinese Academy of Sciences,

Guangzhou, 510650

China

E-mail: caohl@scib.ac.cn

Running title: Microsatellites in *Aquilaria sinensis*

Key words: *Aquilaria crassna*; *A. yunnanensis*; conservation genetics; genetic diversity; molecular markers; RAD-seq

Introduction

Aquilaria sinensis (Thymelaeaceae) is an economically important evergreen tree endemic to South China (Jim 2015). Its wood can produce agarwood, called "Chen Xiang" in Chinese, which is a famous resin used for incense and Chinese traditional medicine (Zhang *et al*. 2012). *Aquilaria sinensis* only produces resin when the wood is wounded by external factors such as worms, wind breaking branches, fungal infections or artificially by drilling holes or cutting the bark (Zhang *et al*. 2012). Because the components of agarwood cannot be produced artificially and are in great demand in the markets (Xu *et al*. 2014), over harvesting highly threatens its population stabilization in the wild (Jim 2015; Chen *et al*. 2016). Nowadays, *A. sinensis* has been listed as a vulnerable species by IUCN (http://www.iucnredlist.org).

In south China, urban development is another threat to *A. sinensis*. It has greatly destroyed the original habitats of *A. sinensis* and resulted in this species found mostly in highly fragmented small *Feng Shui* (geomantic) woodlands. Because habitat fragmentation has a strong negative impact on the genetic structure of species (Young *et al*. 1996; Frankham 2015), conservation studies are urgently needed to improve our ability to make relevant recommendations on ways to alleviate the negative impacts of urban development on this native and precious species. In this process, we will not only investigate the genetic diversity and structure of *A. sinensis* within and among populations, but also conduct parentage analysis to detect real time gene flow, identify mating system within population and possible urban landscapes impeding gene flow among populations.

To achieve these goals, microsatellite markers are the most suitable tools due to their high polymorphism. As only a few microsatellite loci are available (Zhang *et al*. 2010), we developed 18 microsatellite markers for *A. sinensis* in this study. We also used them to evaluate cross-species amplification in two other *Aquilaria* species, *A. yunnanensis* and *A. crassna*. *Aquilaria yunnanensis* is another endemic species in China. With *A. sinensis*, they are the only two *Aquilaria* species naturally distributed in China. To our knowledge, this is the first report of microsatellite loci in *A. yunnanensis* by cross-amplification. *Aquilaria crassna*, another IUCN listed endangered species, naturally grows in South Asia including Cambodia, Lao People's Democratic Republic, Thailand and Viet Nam. *Aquilaria crassna* is also an important agarwood producing tree and the only

Aquilaria species planted in China. Therefore, microsatellite markers developed by cross-species amplification in *A. crassna* would be valuable for its provenience identification and genetic resource management.

Materials and methods

We used restriction site-associated DNA sequencing (RAD-seq) method to obtain the whole genome DNA sequences of *A. sinensis*. Based on these sequences, microsatellites were then identified and characterized.

Leaf samples from one *A. sinensis* individual in South China Botanical Garden were collected. Following the methods of Baird *et al*. (2008), we prepared RAD-seq libraries with restriction enzyme *EcoR*I followed by 150-bp paired-end sequencing with Illumina HiSeq 2500 genetic analyzer. We then obtained a total of 61,613,346 raw reads. The raw sequence data are available in NCBI SRA database with accession number SRX3769703. Filtering PCR duplicates and low-quality reads resulted in 34,219,950 useful reads. We assembled these sequences using the Rainbow 2.0.4 (Chong *et al.* 2012) and used Msatcommander 0.8.2 (Faircloth 2008) to screen microsatellites from these assembled sequences. Particularly, we only chose sequences with their dinucleotide and trinucleotide motifs having at least eight repeats, and we then randomly chose 100 microsatellite sequences from them. We performed PCRs to test the availability of these microsatellites by the same PCR procedures of Wang *et al*. (2007) but with annealing temperature of 55°C for all microsatellite loci. After checking PCR products on 2% agarose gels, we found that 35 microsatellites could be successfully amplified with the right size. Because agarose gels could not separate polymorphic alleles well in microsatellites, initially we used six individuals from Dinghushan reserve (DHS, 112°30'39"E, 23 °09' 21"N), in Guangdong province China, to perform PCR and identify their polymorphism. After PCR amplification and running PCR products on ABI 3730 sequencer (Applied Biosystems, Carlsbad, CA, USA), we obtained a total of 25 microsatellites that gave clear polymorphism for these six individuals. For these microsatellites, we used additional 74 individuals from DHS (21 individuals), Jichilin (JCL, 26 individuals, 113°50'46"E, 22°56'37"N) and Lufushan (LFS, 27 individuals, 114°00'59"E, 23°17'00"N) to identify their full range of allele variation. Finally, we obtained 18 microsatellites which gave unambiguously polymorphic patterns

across populations (Table 1). We also collected 27 samples of *A. crassna* from Boluo (BL, 114°17'22"E, 23°10'20"N), Guangdong province and 24 samples of *A. yunnanensis* from XiShuangbanna (101°34'35"E, 21°36'50"N), Yunnan province, China, to test cross-compatibility for these 18 loci. These sampling sites were illustrated in figure 1.

We calculated genetic diversity parameters, allelic richness (*A*), observed and unbiased expected heterozygosity (H_O, H_E) using GenAlEx 6.501 (Peakall and Smouse 2012), and the fixation index (*f*) using GENEPOP 4.3 (Rousset 2008). Because the number of alleles depends on sample size, making the allelic richness results difficult to compare among species/populations, ADZE 1.0 software (Szpiech *et al*. 2008) was further used to compute rarefied allelic richness controlling for sample sizes. We also used GENEPOP 4.3 to assess the deviation from Hardy-Weinberg equilibrium (HWE) and genotypic linkage disequilibrium (LD) among all pairs of loci. The levels of significance for HWE and LD were adjusted by using the sequential Bonferroni correction (Holm 1979). Then, we used principle coordinate analysis (PCoA) in GenAlEx 6.501 to visualize the genetic relationships among the three *Aquliaria* species and three *A. sinensis* populations in this study.

Results and discussion

The *de novo* assembly of our RAD-seq reads using Rainbow program resulted in 884,053 contigs with a total assembly length of 196,652,287 bp. The minimum and maximum lengths of contigs were 80 bp and 888 bp, respectively, with an average length of 222.44 bp and a N50 of 320 bp. According to our recent whole genome sequencing results using 150-bp paired-end library generated on Illumina HiSeq X Ten platform (unpublished data), the genome size of *A. sinensis* is estimated to be 560 Mb based on the 21-mer analysis. Therefore, the assembled sequences roughly represented 35% of the estimated *A. sinensis* genome. We finally obtained 8,432 sequences containing dinucleotide repeat motifs and 1,392 containing trinucleotide repeat motifs, but only 1,014 of these sequences containing appropriate flanking regions to design primers.

For 100 randomly chosen microsatellite sequences, a total of 18 polymorphic microsatellite markers were identified for *A. sinensis* (tables 1 and 2); they were all successfully amplified in *A. crassna*, but only 17 of them could be amplified in *A. yunnanensis* (table 3); and the 18 loci for *A. crassna* and 13 of the 17 loci for *A. yunnanensis* were polymorphic. Because cross-species

amplification in microsatellite loci was more likely to be successful for genetically more related than for less related species, our cross-amplification results indicated that *A. sinensis* and *A. crassna* were genetically closer to each other than *A. yunnanensis* to them. Only two loci, TCX-18 and TCX-67, exhibited significant departure from HWE in DHS population. No locus pairs showed consistently significant linkage disequilibrium across populations after Bonferroni correction.

At population level for *A. sinensis*, the number of alleles per locus varied from 1 to 10 (table 2), and among all the loci, locus TCX-40 had the highest number of alleles in all three populations studied. It also had the highest number of alleles in *A. crassna* with a value of 8 (table 3). However, besides locus TCX- 40, loci TCX-27 and TCX-61 also exhibited the same highest number of alleles in *A. yunnanensis*. The polymorphism of locus TCX-22 was detected in DHS but not in JCL and LFS populations of *A. sinensis*. Rarefaction curves of allelic richness obtained by the 18 microsatellite loci showed that the DHS population had the highest allelic richness and the LFS population the lowest for *A. sinensis*, and the JCL population of *A. sinensis* and *A. crassna* and *A. yunnanensis* populations showed moderate allelic richness (figure 2).

The H_O and H_E of *A. sinensis* populations varied from 0.000 to 0.926 and from 0.000 to 0.858, respectively (table 2). Locus TCX-40 had both the highest H_O, 0.926 and 0.846, and H_E values, 0.858 and 0.795, for populations DHS and JCL, respectively. In LFS population, the highest H_O (0.926) was also observed in locus TCX-40, but the highest H_E (0.745) occurred in locus TCX-65. Locus TCX-40 showed the highest H_E in both *A. crassna* and *A. yunnanensis* populations, but the highest H_O occurred in locus TCX-12 for *A. crassna* and in three loci, TCX-10, TCX-40 and TCX-61, in *A. yunnanensis* (table 3). Among the three *A. sinensis* and two *A. crassna* and *A. yunnanensis*. populations, the DHS population of *A. sinensis* had the highest H_O and H_E (table 2 and 3). Therefore, these and the allelic richness results together indicate that the DHS population of *A. sinensis* harbored the highest genetic diversity. This is not surprising as the DHS is a nature reserve which has been conserved for more than 400 years (Wang *et al*. 2016), with the longest conservation history than the other sampling sites. In history, south China frequently suffered from severe deforestation which greatly reduced population sizes for local forest tree species including *A. sinensis* in less protected area. Deforestation also results in habitat fragmentation threating *A. sinensis* population health and sustainability (Zou *et al*. 2012). Additionally, as *A. sinensis* is economically important,

overexploitation has seriously threatened its populations continually (Jim 2015). All these factors definitely led to loss of genetic diversity in *A. sinensis* populations, especially in less protected areas (Zou *et al*. 2012). Healthy *A. sinensis* populations can only be maintained in well protected areas, such as DHS reserve. DHS reserve was established in 1956 and is the first nature reserve in China. Due to its rich biodiversity, it was then chosen as one of the Biosphere Reserves of the MAB programs of UNESCO in 1979. However, long before these, DHS had become a famous Buddhist place as early as Ming Dynasty (17 century), and the local vegetation could be well protected by monks since then. In the field, compared to the other sampling sites such as JCL and LFS where the population size was small (< 200 individuals for each site), population size of *A. sinensis* in DHS was obviously large (>2000 individuals personal observation). Large population size will greatly buffer genetic diversity loss through deterring harmful genetic, demographic or/and stochastic effects (Young *et al*. 1996; Frankham 2015). Therefore, the highest genetic diversity in DHS population of *A. sinensis* could be attributable to low level of artificial disturbing in this population.

Plot by the first and second PCoA components for all three *A. sinensis* and two *A. crassna* and *A. yunnanensis* populations indicated that *A. yunnanensis* was well separated from the rest by PCoA 1 that accounted for about 3 times as much variation as PCoA 2 (figure 3). It indicated that *A. yunnanensis* was more genetically different from both *A. sinensis* and *A. crassna* than *A. crassna* and *A. sinensis* from each other. These were consistent to our loci cross-amplification results described above. Phylogenetically, the genetic differences among *A. sinensis*, *A. crassna* and *A. yunnanensis* depended on DNA sequence combinations used (Lee *et al*. 2016). Lee *et al*. (2016) reported that the results from each of trnL-trnF+ITS, trnL-trnF+ITS2, trnL-trnF+psbA-trnH+ITS2 and rbcL+trnL-trnF+ITS loci combinations showed that *A. sinensis* and *A. crassna* were genetically closer to each other than they were to *A. yunnanensis*, but those from *mat*K+*trn*L-*trn*F+ITS2 loci combination showed *A. sinensis* and *A. yunnanensis* were genetically closer to each other than they were to *A. crassna*. Although they did not give explanations for these inconsistent results among the three *Aquilaria* species we studied, our microsatellite cross-amplification and PCoA results provided additional information for the phylogenetic studies. Consistent with our results, leaf anatomical structure analysis also indicated that *A. sinensis* and *A. crassna* were more morphologically similar than they were to *A. yunnanensis* (Liu *et al*. 2017), suggesting that these

two species may have only diverged recently. However, further investigations taking their origins into consideration are needed to study this possibility.

We reran PCoA without *A. yunnanensis*. The PCoA plot using the PCoA 1 and 2 from this rerun showed that the individuals from *A. crassna* and all three *A. sinensis* populations were well grouped to their origins and these groups were similarly separated from each other (figure 4), indicating the genetic differentiation among the three *A. sinensis* populations was similar with that between *A. crassna* and *A. sinensis* species. Therefore, genetic differentiation among the *A. sinensis* populations might be high. Using ISSR (inter-simple sequence repeat) and SRAP (sequence-related amplified polymorphism) markers, Zhou *et al*. (2012) indicated that restricted gene flow among populations resulted in high genetic differentiation. Reproductive study showed that *A. sinensis* was an insect (such as noctuids and pyralids) pollinated and seed insect (hornets) dispersed species (Chen *et al*. 2016). Such gene flows by insects were distance-limited and might have contributed to the high genetic differentiation among *A. sinensis* populations we observed.

Overall, 18 polymorphic microsatellites of *A. sinensis* were isolated and tested, and they were also successfully amplified in *A. crassna* and 17 of them in *A. yunnanensis*. These microsatellites will be useful to study and understand the effects of habitat fragmentation on the genetic diversity and structure in *A. sinensis* populations for the sustainable management of this species. Furthermore, to our knowledge, it is the first time to report microsatellite loci in *A. yunnanensis* by cross-amplification.

Acknowledgements

We thank all editors and reviewers for their valuable comments on the manuscript. This study is supported by Science and Technology Project of Dongguan city (2015108101002), Conservation of traditional Chinese medicine by Forestry Administration of Guangdong, Special foundation for conservation of wild animals, plants and wetlands by Forestry Administration of Guangdong (2130299), Science and Technology Project of Guangdong Province (2017A030303060), Project for conservation and management of wild animals and plants in Guangdong province.

References

Baird N. A., Etter P. D., Atwood T. S., Currey M. C., Shiver A. L., Lewis Z. A. *et al.* 2008 Rapid SNP discovery and genetic mapping using sequenced RAD markers. *PLoS ONE* **3**, e3376.

Chen G., Liu C. and Sun W. 2016 Pollination and seed dispersal of *Aquilaria sinensis* (Lour.) Gilg (Thymelaeaceae): An economic plant species with extremely small populations in China. *Plant divers*. **38**, 227-232.

Chong Z., Ruan J. and Wu C. I. 2012 Rainbow: an integrated tool for efficient clustering and assembling RAD-seq reads. *Bioinformatics* **28**, 2732-2737.

Faircloth B. C. 2008 MSATCOMMANDER: detection of microsatellite repeat arrays and automated, locus-specific primer design. *Mol. Ecol. Resour.* **8**, 92-94.

Frankham R. 2015 Genetic rescue of small inbred populations: meta-analysis reveals large and consistent benefits of gene flow. *Mol. Ecol*. 24, 2610-2618.

Holm S. 1979 A simple sequentially rejective multiple test procedure. *Scand. J. Stat.* **6**, 65-70.

Jim C. Y. 2015 Cross-border itinerant poaching of agarwood in Hong Kong's peri-urban forests. *Urban For. Urban Gree.* **14**, 420-431.

Lee S. Y., Ng W. L., Mahat M. N., Nazre M. and Mohamed R. 2016 DNA barcoding of the endangered *Aquilaria* (Thymelaeaceae) and its application in species authentication of agarwood products traded in the market. *PLoS ONE* **11**, e0154631.

Liu P., Zhang Y., Yang Y. and Chen B. 2017 Leaf anatomical structure of six *Aquilaria* species. *Guihaia* **37**, 565-571.

Peakall R. and Smouse P. 2012 GenAlEx 6.5: Genetic analysis in Excel. Population genetic software for teaching and research - an update. *Bioinformatics* **28**, 2537-2539.

Rousset F. 2008 GENEPOP'007: a complete re-implementation of the genepop software for Windows and Linux. *Mol. Ecol. Resour.* **8**, 103-106.

Szpiech Z. A., Jakobsson M. and Rosenberg N. A. 2008 ADZE: a rarefaction approach for counting alleles private to combinations of populations. *Bioinformatics* **24**, 2498-2504.

Wang Z. F., Li G, Fu S. L. and Ren H. 2007 Isolation and characterization of microsatellite loci in *Cryptocarya chinensis* in lower subtropical China. *Conserv. Genet.* **8**, 1235-1237.

Wang Z. F., Lian J. Y., Ye W. H., Cao H. L., Zhang Q. M. and Wang Z. M. 2016 Pollen and seed flow under different predominant winds in wind-pollinated and wind-dispersed species *Engelhardia roxburghiana*. *Tree genet. Genomes* **12**, 19.

Xu Y., Liu J., Liang L., Yang X., Zhang Z., Gao Z. *et al.* 2014 Molecular cloning and characterization of three cDNAs encoding 1-deoxy- D -xylulose-5-phosphate synthase in *Aquilaria sinensis* (Lour.) Gilg. *Plant Physiol. Bioch.* **82**, 133-141.

Young A., Boyle T. and Brown T. 1996 The population genetic consequences of habitat fragmentation for plants. *Trends Ecol. Evol.* **11**, 413-418.

Zhang X. L., Liu Y. Y., Wei J. H., Yang Y., Zhang Z., Huang J. Q. *et al.* 2012 Production of high-quality agarwood in *Aquilaria sinensis* trees via whole-tree agarwood-induction technology. *Chinese Chem. Lett.* **23**, 727-730.

Zhang Y. T., Wang Z. F., Cao H. L., Li X. Y., Wu L. F., Zhuo S. B. *et al.* 2010 Isolation and characterization of polymorphic microsatellite loci in *Aquilaria sinensis* (Lour.) Gilg. *Conserv. Genet. Resour.* **2(Supplement 1)**, 5-6.

Zou M., Xia Z, Lu C., Wang H., Ji J. and Wang W. 2012 Genetic Diversity and Differentiation of *Aquilaria sinensis* (Lour.) Gilg Revealed by ISSR and SRAP Markers. *Crop Sci.* **52**, 2304-2313.

Received 17 October 2017; revised 7 April 2018; accepted 11 April 2018

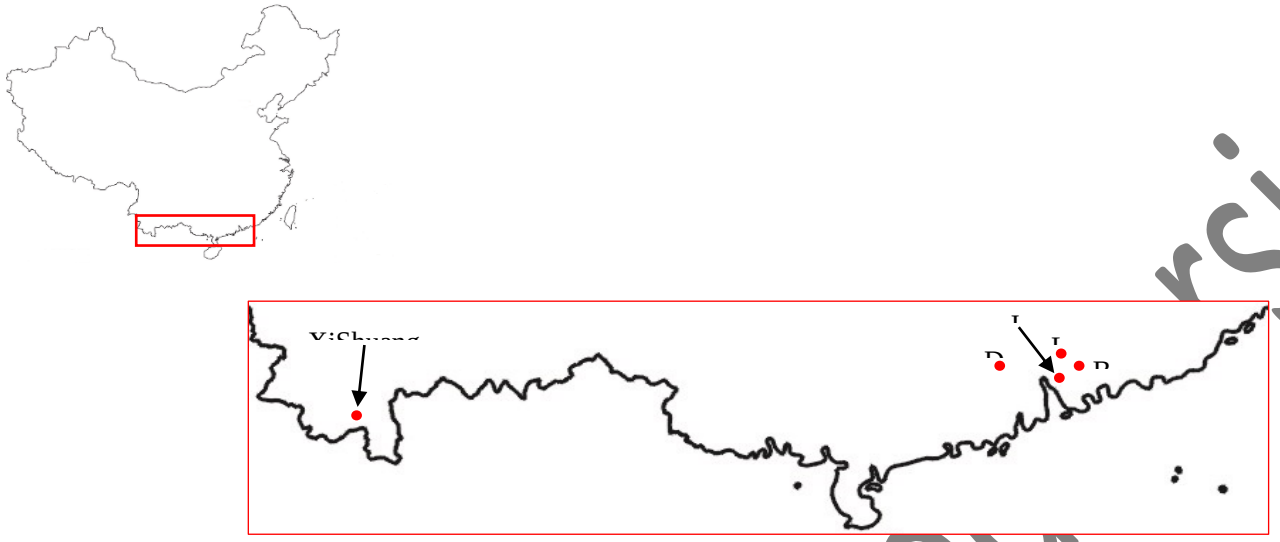

Figure 1. Map showing sampling sites for three *Aquilaria sinensis* populations (DHS, JCL and LFS), *A. crassna* (BL) and *A. yunnanensis* (Xishuangbanna).

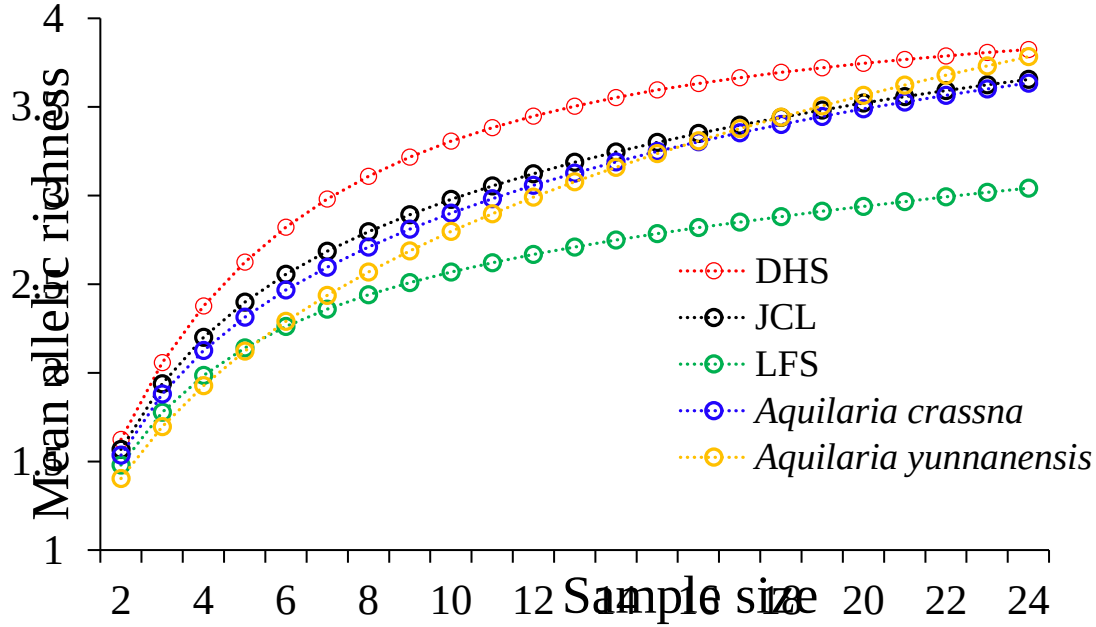

Figure 2. Rarefaction curves of allelic richness calculated by ADZE for three *Aquilaria sinensis* populations, *A. crassna* and *A. yunnanensis*.

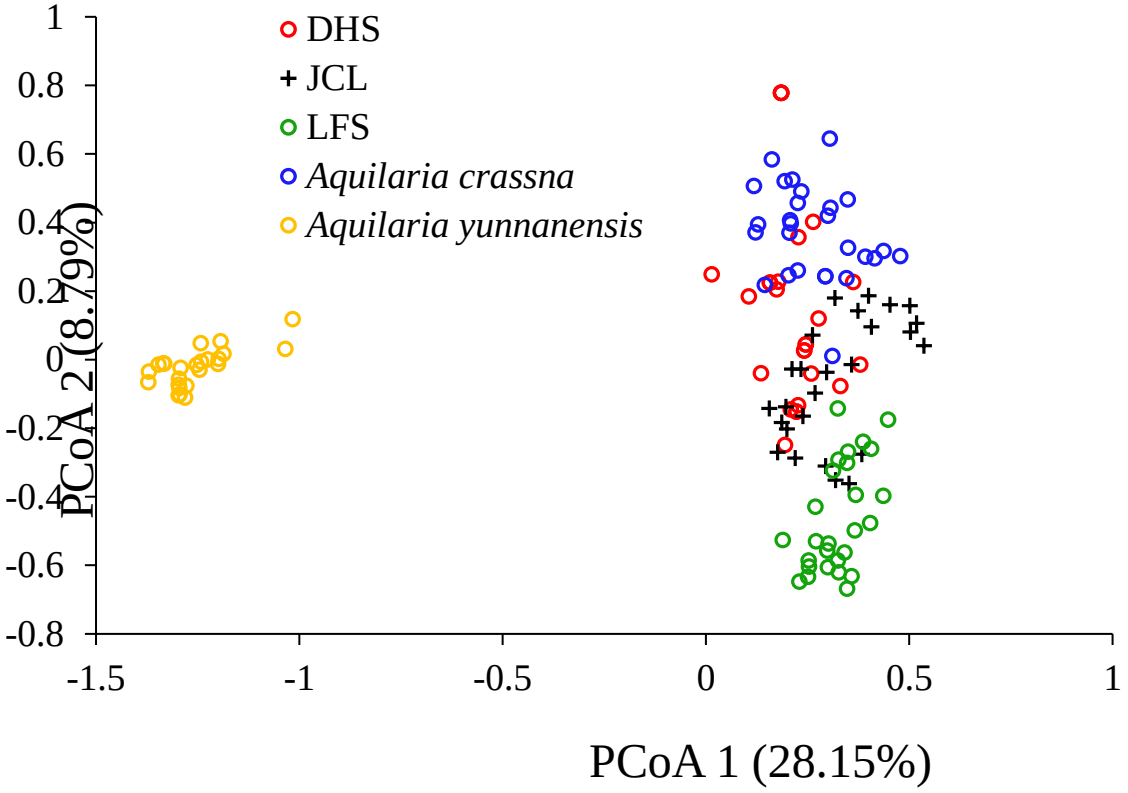

Figure 3. Principal coordinate plot of three *A. sinensis* populations, and two *A. crassna* and *A. yunnanensis* populations.

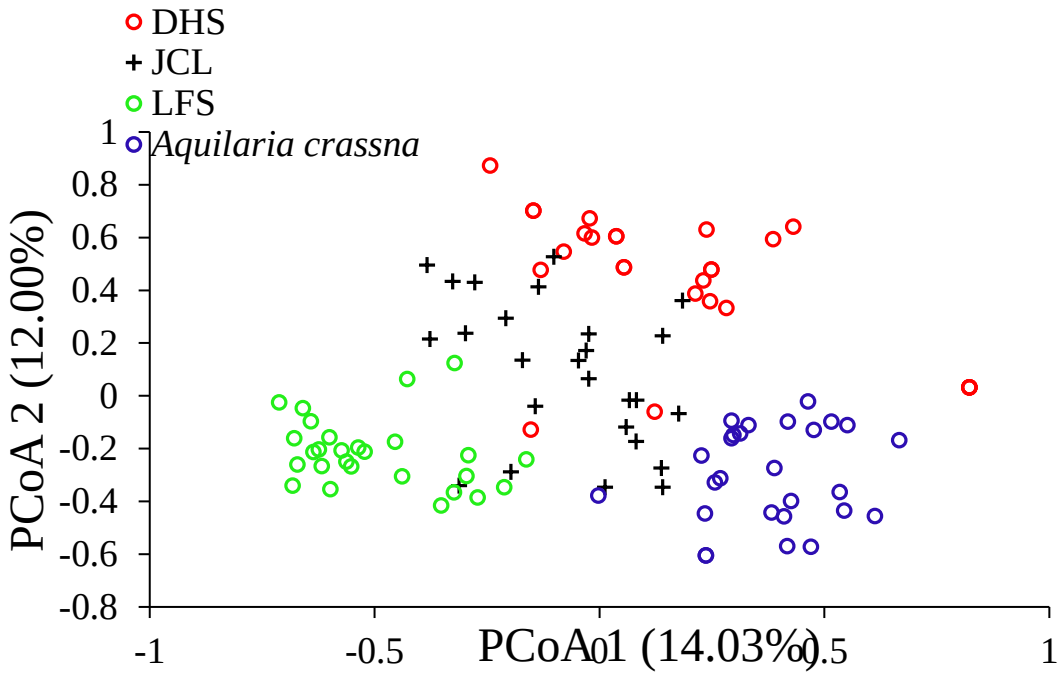

Figure 4. Principal coordinate plot of three *Aquilaria sinensis* populations and one *A. crassna* population.

Table 1. Characteristics of 18 microsatellite markers developed in *Aquilaria sinensis.* Annealing temperature was for 55°C for all loci.

Locus	Repeat motifs of individual applied to RAD sequencing	Primer sequences (5'-3')	Size range (bp)	GENBANK accession No.
TCX-10	$(CT)_7GT(CT)_3(AC)_{14}$	F: FAM-TCATTAGTTAGGGATGTCCCAC R: GTTCCAATCAGCCATGAGCC	143−190	KY304005
TCX-12	$(AG)_9$	F: FAM-ACTAAGGTTTGGAACATACTGGC R: GGTGTTGAGCCTGCTGAAAG	313−325	KY304006
TCX-16	$(TC)_{11}$	F: FAM-AAGCACTAGGTTCTTTAGTTCAC R: TGATTCTACATTTGATTGTGGCG	156−170	KY304007
TCX-18	$(CA)_9$	F: FAM-GGATCAAAGATGCCGAATGC R: GTTTGGGCTCATGTCCACG	338−356	KY304008
TCX-20	$(ATT)_{14}$	F: FAM-TGGACGAACAACACTTATTGGC R: GGCGGATCGCTTGGATTTC	246−273	KY304010
TCX-22	$(TCC)_8$	F: FAM-CAAGTTCCGACCATAACCCG R: CGCTTTGCGGTTCTCAGG	246−255	KY304011
TCX-27	$(CT)_9$	F: FAM-TGATTGACCCTCTTCCTGGC	253−259	KY304012

		R: AGCTAGACAGAATCCCTAATATTGC		
TCX-39	$(GA)_8$	F: FAM-GGTTCAGTTGCTTAGTGGGC R: ACGTGCCGGAGTGGTTATC	175−179	KY304014
TCX-40	$(AT)_{11}$	F: FAM-GCTTTAGGGAAAGGCTACGG R: CTGTCGCTCACTCGTTTAGG	145−229	KY304015
TCX-42	$(TG)_9$	F: FAM-ACACATGCTAGGGCTTCGG R: TACCCACTCCGGCGTAGAC	220−224	KY304016
TCX-43	$(CT)_{12}$	F: FAM-AGACACCAAAGAGCCAAGC R: TCACCTCCATTCTTCCACCG	180−186	KY304017
TCX-53	$(CCT)_{10}$	F: FAM-ATCCTGCCCTTCTCGGTTG R: GGTAGCCACCTCGTACTGG	194−197	KY304018
TCX-61	$(CT)_{15}$	F: FAM-AGGAGATCAAATCCAGCTAGTC R: TGATCCCTCATTCACATGGC	222−234	KY304020
TCX-64	$(GA)_{13}$	F: FAM-TTTGCGTTTGCCTAGAGCC R: CTGGTTGAGCGGCCTTTAC	200−214	KY304021
TCX-65	$(CT)_{10}$	F: FAM-TGTTTGTTCATGCGGGACG R: GTCGCTTCGATCTGCCAAG	181−195	KY304022

TCX-67	$(TA)_{11}$	F: FAM-AAATGGATTCCCGCGCTTC R: GGATGTTTAGAGGCTAACAAATATACG	300−308	KY304023
TCX-83	$(TGA)_{9}$	F: FAM-CCACTAACCGAAGTTGGATGC R: TCTGTTTCTTCGCCCCACC	172−175	KY304027
TCX-91	$(CT)_{18}$	F: FAM-ACGCTCTTTAAACCGAAACCTC R: GAGTGGCTGCTTTGTGGC	150−182	KY304028

Table 2. Genetic diversities of 18 microsatellites in three populations of *Aquilaria sinensis*.

Locus	DHS (n=27)				JCL (n=26)				LFS (n=27)			
	A	H_O	H_E	*f*	*A*	H_O	H_E	*f*	*A*	H_O	H_E	*f*
TCX-10	5	0.741	0.667	-0.112	6	0.731	0.728	-0.004	5	0.519	0.495	-0.048
TCX-12	3	0.259	0.343	0.248	5	0.423	0.400	-0.060	3	0.259	0.237	-0.096
TCX-16	6	0.852	0.816	-0.045	4	0.538	0.633	0.152	5	0.556	0.574	0.032
TCX-18	3	0.185	0.440	0.583*	3	0.192	0.215	0.107	3	0.111	0.108	-0.026
TCX-20	4	0.481	0.389	-0.245	6	0.600	0.680	0.120	4	0.538	0.506	-0.065
TCX-22	2	0.630	0.465	-0.364	1	0.000	0.000	-	1	0.000	0.000	-
TCX-27	3	0.741	0.624	-0.191	3	0.538	0.539	0.001	3	0.296	0.371	0.205
TCX-39	3	0.556	0.645	0.141	3	0.538	0.544	0.010	3	0.556	0.526	-0.057
TCX-40	10	0.926	0.858	-0.081	8	0.846	0.795	-0.066	7	0.926	0.728	-0.278
TCX-42	3	0.593	0.507	-0.174	2	0.231	0.208	-0.111	2	0.148	0.140	-0.061
TCX-43	2	0.556	0.440	-0.270	3	0.615	0.571	-0.080	3	0.593	0.589	-0.006
TCX-53	2	0.444	0.352	-0.268	2	0.500	0.473	-0.059	2	0.481	0.372	-0.300
TCX-61	3	0.630	0.590	-0.068	4	0.500	0.569	0.124	3	0.667	0.635	-0.052
TCX-64	3	0.778	0.626	-0.248	4	0.500	0.542	0.079	3	0.407	0.381	-0.071

TCX-65	6	0.926	0.783	-0.187	6	0.500	0.713	0.303	5	0.741	0.745	0.006
TCX-67	4	0.926	0.697	-0.337*	4	0.400	0.626	0.366	4	0.111	0.109	-0.020
TCX-83	2	0.481	0.465	-0.037	2	0.500	0.503	0.006	2	0.074	0.073	-0.020
TCX-91	6	0.778	0.716	-0.089	5	0.692	0.701	0.012	3	0.556	0.637	0.130
Overall	-	0.638	0.579	-0.104	-	0.491	0.524	0.063	-	0.419	0.401	-0.044

A: number of alleles; H_O: observed heterozygosity; H_E: unbiased expected heterozygosity; *f*: fixation index

*P<0.05 after the Bonferroni correction

Table 3. Cross-amplification of 18 microsatellites in *Aquilaria crassna* and *A. yunnanensis*.

Locus	*A. crassna* (n=27)				*A. yunnanensis* (n=24)			
	A	H_O	H_E	*f*	*A*	H_O	H_E	*f*
TCX-10	5	0.630	0.584	-0.080	6	0.917	0.709	-0.301
TCX-12	4	0.815	0.727	-0.124	5	0.652	0.636	-0.026
TCX-16	5	0.630	0.667	0.058	4	0.292	0.329	0.115
TCX-18	2	0.519	0.509	-0.020	4	0.417	0.418	0.002
TCX-20	5	0.333	0.331	-0.009	9	0.913	0.798	-0.148
TCX-22	2	0.370	0.352	-0.053	5	0.500	0.605	0.176
TCX-27	3	0.074	0.073	-0.010	11	0.875	0.833	-0.051
TCX-39	4	0.593	0.572	-0.036	1	0.000	0.000	-
TCX-40	8	0.808	0.791	-0.021	11	0.917	0.863	-0.064
TCX-42	3	0.630	0.534	-0.183	-	-	-	-
TCX-43	4	0.778	0.667	-0.169	1	0.000	0.000	-
TCX-53	4	0.630	0.618	-0.020	1	0.000	0.000	-
TCX-61	5	0.704	0.535	-0.323	11	0.917	0.823	-0.117
TCX-64	4	0.519	0.645	0.199	1	0.000	0.000	-
TCX-65	6	0.704	0.637	-0.106	3	0.708	0.520	-0.372
TCX-67	6	0.630	0.653	0.036	8	0.864	0.730	-0.188
TCX-83	2	0.370	0.307	-0.209	2	0.045	0.045	0.000
TCX-91	4	0.519	0.549	0.056	1	0.000	0.000	-
Overall	-	0.570	0.542	-0.052	-	0.445	0.406	-0.098*

A: number of alleles; H_O: observed heterozygosity; H_E: unbiased expected heterozygosity; *f*: fixation index

*P<0.05 after the Bonferroni correction